Reversal of Obesity- and Diet-Induced Insulin Resistance with Salicylates or Targeted Disruption of *Ikkβ*

Minsheng Yuan,[1]* Nicky Konstantopoulos,[1]* Jongsoon Lee,[1]* Lone Hansen,[1] Zhi-Wei Li,[2] Michael Karin,[2] Steven E. Shoelson[1]†

We show that high doses of salicylates reverse hyperglycemia, hyperinsulinemia, and dyslipidemia in obese rodents by sensitizing insulin signaling. Activation or overexpression of the IκB kinase β (IKKβ) attenuated insulin signaling in cultured cells, whereas IKKβ inhibition reversed insulin resistance. Thus, IKKβ, rather than the cyclooxygenases, appears to be the relevant molecular target. Heterozygous deletion (*Ikkβ*$^{+/-}$) protected against the development of insulin resistance during high-fat feeding and in obese *Lep*$^{ob/ob}$ mice. These findings implicate an inflammatory process in the pathogenesis of insulin resistance in obesity and type 2 diabetes mellitus and identify the IKKβ pathway as a target for insulin sensitization.

Insulin resistance refers to a decreased capacity of circulating insulin to regulate nutrient metabolism. Individuals with insulin resistance are predisposed to developing type 2 diabetes, and insulin resistance is an integral feature of its pathophysiology. Chronic secretion of large amounts of insulin to overcome tissue insensitivity can lead, in predisposed individuals, to pancreatic β cell failure and concomitant defects in glucose and lipid metabolism. The prevalence of insulin resistance is high and rising, but only rare genetic causes have been identified. The molecular cause of acquired insulin resistance, which is promoted by sedentary lifestyle, obesity, fatty diet, and increased age, and is reversed by exercise and weight loss, is similarly unknown.

High doses of salicylates [4 to 10 g per day (g/day)], including sodium salicylate and aspirin, have been used to treat inflammatory conditions such as rheumatic fever and rheumatoid arthritis. These high doses are thought to inhibit nuclear factor kappa B (NF-κB) (*1*) and its upstream activator the IκB kinase β (IKKβ) (*2*), as opposed to working through cyclooxygenases (COXs), the classical targets of nonsteroidal anti-inflammatory drugs (NSAIDs). High doses of salicylates also lower blood glucose concentrations (*3*–*7*), although their potential for treating diabetes has been all but forgotten by modern biomedical science. We have investigated potential mechanisms of these hypoglycemic effects to identify potential mediators of insulin resistance and molecular targets for intervention. We have found that reduced signaling through the IKKβ pathway, either by salicylate inhibition or decreased IKKβ expression, is accompanied by improved insulin sensitivity in vivo. Our findings further indicate that the IKKβ pathway may contribute to insulin resistance in type 2 diabetes and obesity by impinging on insulin signaling.

We determined the effect of high doses of salicylates on the severe insulin resistance seen in genetically obese rodents. Twelve-week-old male Zucker *fa/fa* rats and 8-week-old male *ob/ob* mice were treated for 3 to 4 weeks with 120 mg/kg/day of aspirin or sodium salicylate, administered by continuous subcutaneous infusion. Fasting blood glucose values and glucose tolerance were improved in Zucker *fa/fa* rats (Fig. 1A). Concomitant reductions in insulin concentrations (Fig. 1B) indicated a marked improvement in insulin sensitivity. Glucose tolerance in lean *fa/+* animals was normal, and blood glucose concentrations were similar after aspirin treatment (Fig. 1C). Nevertheless, lower insulin concentrations in the aspirin-treated group (Fig. 1D) demonstrate improved insulin sensitivity, despite milder insulin resistance. The ability of high-dose aspirin to increase insulin sensitivity was further established in insulin tolerance tests (Fig. 1E). Intraperitoneal injection of insulin (2.0 U per kilogram of body weight) had essentially no effect on blood glucose concentrations in untreated *fa/fa* rats. However, the same insulin dose caused a decrease in blood glucose when given to aspirin-treated animals.

Increased triglyceride concentrations in the blood of Zucker rats fell from 494 ± 68 mg/dl to 90 ± 58 mg/dl during 3 weeks of

[1]Joslin Diabetes Center and Department of Medicine, Harvard Medical School, Boston, MA 02215, USA. [2]Department of Pharmacology, University of California, San Diego, La Jolla, CA 92093, USA.

*These authors contributed equally to this work.
†To whom correspondence should be addressed. E-mail: Steven.Shoelson@Joslin.Harvard.edu

References and Notes

1. L. M. Eisenberg, R. R. Markwald, *Circ. Res.* **77**, 1 (1995).
2. C. B. Brown, A. S. Boyer, R. B. Runyan, J. V. Barnett, *Science* **283**, 2080 (1999).
3. _____, *Dev. Biol.* **174**, 248 (1996).
4. A. S. Boyer *et al.*, *Dev. Biol.* **208**, 530 (1999).
5. Y. Nakajima, T. Yamagishi, S. Hokari, H. Nakamura, *Anat. Rec.* **258**, 119 (2000).
6. D. Y. Stainier *et al.*, *Development* **123**, 285 (1996).
7. L. S. Motoike *et al.*, *Genesis* **28**, 75 (2000).
8. J. H. Postlethwait, W. S. Talbot, *Trends Genet.* **13**, 183 (1997).
9. Haploid wild-type and diploid mutant embryos from AB/SJD hybrids were genotyped for agarose polymorphisms with z1154, z20950, and z6974, as well as for a single-strand conformation polymorphism (SSCP) (*35*) in the 3′-untranslated region of *ldb3*.
10. The coding sequence mutation in *ugdh* was determined by sequencing wild-type and mutant cDNA clones isolated with primers designed from zebrafish EST sequence information (fc15f10 *ugdh* EST, GenBank accession number AI657608). Mutations were confirmed by dCAP-based RFLP generated by the T to A substitution at base pair 992 using the primers 5′-GACATGAATGAATATCAGAGAAAGAG-3′ and 5′-AGGAGAAACCCAACAACGC-3′ and digesting with Mlu I. Oligonucleotides were designed as described (*36*).
11. Supplementary Web material is available on *Science* Online at www.sciencemag.org/cgi/content/full/293/5534/1670/DC1.
12. R. E. Campbell, S. C. Mosimann, I. van De Rijn, M. E. Tanner, N. C. Strynadka, *Biochemistry* **39**, 7012 (2000).
13. A. D. Lander, S. B. Selleck, *J. Cell Biol.* **148**, 227 (2000).
14. X. Lin *et al.*, *Dev. Biol.* **224**, 299 (2000).
15. J. Topczewski *et al.*, *Dev. Cell* **1**, 251 (2001).
16. S. C. Neuhauss *et al.*, *Development* **123**, 357 (1996).
17. Morpholinos designed against zebrafish *ugdh* (5′-TCTTTTTAATCTGAAACATCGTGTC-3′) were injected at 4 ng per embryo.
18. J. Westin, M. Lardelli, *Dev. Genes Evol.* **207**, 51 (1997).
19. C. Thisse, B. Thisse, *Development* **126**, 229 (1999).
20. E. C. Walsh, D. Y. R. Stainier, unpublished data.
21. Y. Chen, G. Struhl, *Cell* **87**, 553 (1996).
22. C. Rodriguez-Esteban *et al.*, *Nature* **386**, 360 (1997).
23. E. Laufer *et al.*, *Nature* **386**, 366 (1997).
24. D. Y. Stainier, B. M. Weinstein, H. W. Detrich, L. I. Zon, M. C. Fishman, *Development* **121**, 3141 (1995).
25. C. Kim, D. Y. R. Stainier, unpublished data.
26. U. Häcker, X. Lin, N. Perrimon, *Development* **124**, 3565 (1997).
27. T. E. Haerry, T. R. Heslip, J. L. Marsh, M. B. O'Connor, *Development* **124**, 3055 (1997).
28. X. Lin, E. M. Buff, N. Perrimon, A. M. Michelson, *Development* **126**, 3715 (1999).
29. R. C. Binari *et al.*, *Development* **124**, 2623 (1997).
30. C. H. Mjaatvedt, H. Yamamura, A. A. Capehart, D. Turner, R. R. Markwald, *Dev. Biol.* **202**, 56 (1998).
31. T. D. Camenisch *et al.*, *J. Clin. Invest.* **106**, 349 (2000).
32. D. Meyer, C. Birchmeier, *Nature* **378**, 386 (1995).
33. K. F. Lee *et al.*, *Nature* **378**, 394 (1995).
34. M. Gassmann *et al.*, *Nature* **378**, 390 (1995).
35. M. Orita, H. Iwahana, H. Kanazawa, K. Hayashi, T. Sekiya, *Proc. Natl. Acad. Sci. U.S.A.* **86**, 2766 (1989).
36. M. M. Neff, J. D. Neff, J. Chory, A. E. Pepper, *Plant J.* **14**, 387 (1998).
37. D. Yelon, S. A. Horne, D. Y. Stainier, *Dev. Biol.* **214**, 23 (1999).
38. M. A. S. Saqi, R. Sayle, *Comput. Appl. Biosci.* **10**, 545 (1994).
39. Whole-mount in situ hybridization was performed as described (*37*). Phenylthiourea (Sigma) was used to inhibit pigmentation in some cases (0.003% w/v).
40. We thank T. Kornberg, A. Javaherian, and members of the lab for discussions and comments on the manuscript; E. Chiang, B.-C. Chung, M. Tada, M.-A. Akimenko, C. Thisse, B. Thisse, and M. Lardelli for providing probes; L. Solnica-Krezel for sharing observations before publication; and M. Fishman for the *m151 jekyll* allele. Supported by a Howard Hughes Predoctoral Fellowship (E.C.W.), the Program in Human Genetics Genomics Core Facility at UCSF, and grants to D.Y.R.S. from the Packard Foundation and the NIH (HL54737).

30 May 2001; accepted 19 July 2001

aspirin treatment (Fig. 1F). The concentrations of free fatty acid (FFA) dropped as well, from 3.1 ± 0.3 mM to 1.1 ± 0.2 mM. The decrease in the amount of circulating FFA occurred within 1 week of aspirin treatment, preceding reductions in the amounts of triglyceride and glucose in the blood. This is consistent with the hypothesis that increased FFA concentrations contribute to the pathogenesis of hyperglycemia and hypertriglyceridemia. Cholesterol concentrations were unaffected. Hepatotoxicity was not observed at the high aspirin and salicylate doses used, judging from the consistently normal circulating concentrations of the liver enzyme alanine aminotransferase (ALT), seen throughout our studies (Fig. 1F). Serum salicylate concentrations were 0.81 ± 0.25 mM.

Ob/ob mice (*Lep*$^{ob/ob}$) are a more relevant model for type 2 diabetes, as the animals are diabetic in addition to being obese and severely insulin-resistant. Fasting blood glucose values and glucose tolerance were significantly improved by aspirin treatment (Fig. 1G). Heterozygous, lean *Lep*$^{ob/+}$ mice exhibited postprandial hyperglycemia but were less insulin resistant. Glucose intolerance in *Lep*$^{ob/+}$ mice was normalized with aspirin treatment (Fig. 1H). Insulin concentrations were reduced during aspirin therapy in both *Lep*$^{ob/ob}$ and *Lep*$^{ob/+}$ mice. Neither aspirin nor salicylate affected food intake or body weight in Zucker *fa/fa* rats or *ob/ob* mice.

We isolated tissues from treated animals to analyze various signaling proteins (*8–10*). Insulin receptor (IR) tyrosine phosphorylation, one of the earliest responses to insulin binding, was barely detectable in the liver and muscle of insulin-resistant Zucker rats (Fig. 2, A and B). Increased stimulation occurred in corresponding tissues from aspirin- and salicylate-treated animals, suggesting an increase in insulin responsiveness. Signaling from the IR to insulin receptor substrates (IRSs), phosphatidylinositol 3-kinase, and the PDK1 protein kinase is required for the maintenance of metabolic homeostasis. Phosphorylation of the protein kinase AKT, a subsequent step in this cascade, correlates with IR activation in tissues from Zucker rats (Fig. 2, A and B). The blunted insulin-stimulated phosphorylation of AKT in the liver and muscle of untreated Zucker rats was increased after aspirin or salicylate treatment, providing a biochemical correlate for increased in vivo insulin sensitivity. The electrophoretic mobility of IRS-1 from rat livers increased with aspirin and salicylate treatment [Web fig. 1 (*11*)], suggesting a decrease in serine-threonine (Ser-Thr) phosphorylation (this is a known inhibitor of insulin signaling). Basal IKK activity was elevated in tissues from Zucker *fa/fa* rats relative to those from lean *fa/+* controls (*12*).

Studies with cultured cells were used to investigate potential mechanisms relating salicylate treatment to the in vivo reversal of insulin resistance. Treatment of 3T3-L1 adipocytes with tumor necrosis factor–α (TNF-α) induced "insulin resistance," as judged by decreases in insulin-stimulated tyrosine phosphorylation of the IR β-subunit and IRS-1, to 42 ± 11% and 37 ± 9%, respectively, of that in insulin-stimulated cells not treated with TNF-α (Fig. 3, A and B) (*13*). This was reversed by prior treatment of cells with high doses of aspirin (5 mM). The amounts of IR and IRS-1 proteins were similar in all cells. TNF-α activates the IKK complex (*14*). Phosphatase inhibitors such as okadaic acid and calyculin A also activate IKKβ (*15*, *16*), but without activating upstream elements in the TNF-α signaling cascade, and these inhibitors also induce insulin resistance in isolated tissues and cultured cells (*17*, *18*). Calyculin A reduced insulin-stimulated tyrosine phosphorylation of the IR and IRS-1, to 29 ± 12% and 16 ± 2%, respectively, of that in untreated cells, and this was prevented by incubating the cells with aspirin (Fig. 3, A

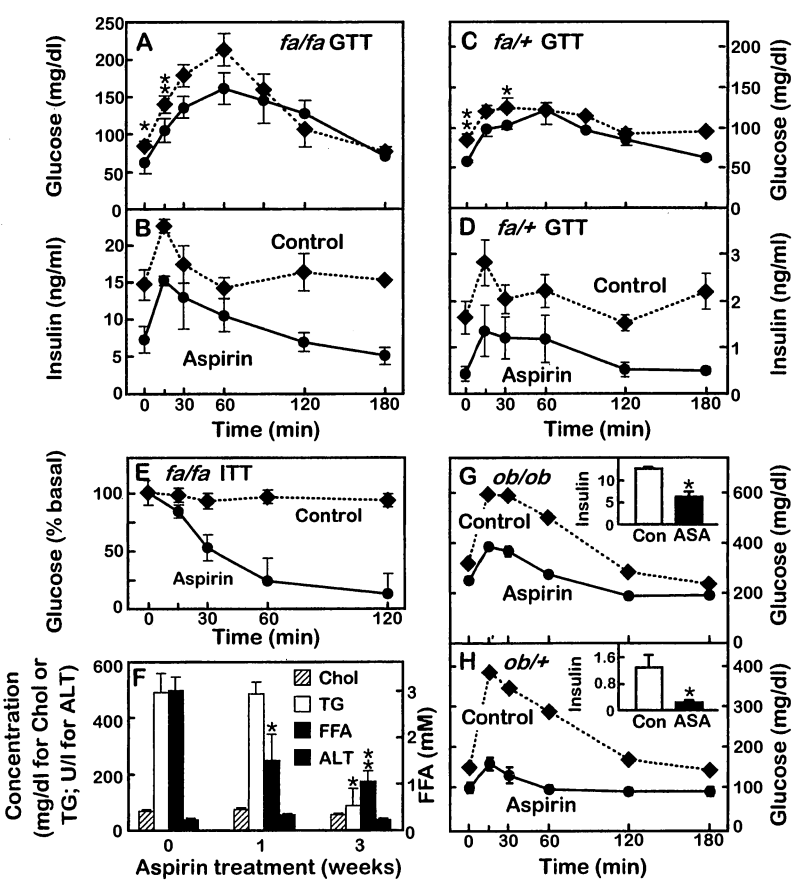

Fig. 1. In vivo effects of aspirin in Zucker fatty rats and *ob/ob* mice. (**A** to **F**) Twelve-week-old male Zucker *fa/fa* rats and (**G** and **H**) 8-week-old *ob/ob* (*Lep*$^{ob/ob}$) and *ob/+* mice were given free access to food and water. Aspirin (120 mg/kg/day) was continuously infused for 3 to 4 weeks by Alzet pumps (pump 2ML2 was used in rats, pump 2002 was used in mice) implanted subcutaneously between the scapulae of the animals. In all panels, data are mean ± SEM values, diamonds and dashed lines represent control implantation of a pump with vehicle only, and solid circles and solid lines represent 3 or 4 weeks of treatment with aspirin. For glucose tolerance tests (GTT), glucose (2.0 g/kg) was administered by oral gavage (rats) or intraperitoneal injection (mice) after an overnight fast. (A and C) Blood glucose and (B and D) serum insulin concentrations were determined during oral glucose tolerance tests in (A and B) Zucker *fa/fa* rats or (C and D) *fa/+* rats; six animals were in each treatment group. In (A) and (C), $*P < 0.05$, $**P < 0.01$ for vehicle versus aspirin treatment, Student's *t* test. (B) $P = 0.0004$ and (D) $P = 0.02$, for vehicle versus aspirin treatment, integrated areas under the curves; Student's *t* test. (E) For insulin tolerance tests (ITT), insulin (2.0 U/kg) was injected intraperitoneally after an overnight fast (six Zucker *fa/fa* rats, $P = 0.0001$, for vehicle versus aspirin treatment, integrated areas under the curves; Student's *t* test). (F) Cholesterol (Chol), triglyceride (TG), long-chain FFA, and ALT concentrations were measured in sera from fasting Zucker *fa/fa* rats (for FFA, $P < 0.005$ for three-group analysis of variance; $*P = 0.01$, $t = 0$ versus $t =$ 1 week of aspirin treatment, $**P < 0.002$, $t = 0$ versus $t =$ 3 weeks of aspirin treatment, Dunnett's adjusted pairwise comparison. For TG, $*P < 0.05$, $t = 0$ versus $t = 3$ weeks of aspirin treatment; Student's *t* tests). Glucose tolerance tests are shown in (G) *ob/ob* and (H) *ob/+* mice. (G) $P = 0.004$ and (H) $P < 0.0001$ for 10 mice treated with vehicle versus 10 mice treated with aspirin, integrated areas under the curves; Student's *t* tests. [Insets in (G) and (H)] Fasting serum insulin concentrations (ng/ml); $**P < 0.01$ for 10 mice treated with aspirin versus 10 controls treated with vehicle alone. Aspirin treatment did not significantly affect food intake or body weights in any of these studies. Animal care was in accordance with institutional and NIH guidelines.

and B). Similar results were obtained after okadaic acid treatment (*19*). The reduced electrophoretic mobility of IRS-1 due to calyculin A treatment was reversed with aspirin (Fig. 3C), further suggesting that aspirin's ability to reverse insulin resistance might result from reduced levels of Ser-Thr phosphorylation of components in the insulin action cascade.

Fao hepatoma cells are an insulin-responsive model for liver as opposed to fat. TNF-α treatment decreased tyrosine phosphorylation of the insulin receptor substrate IRS-2 (Fig. 4A) (*20*). Decreased IRS-2 tyrosine phosphorylation was reversed by aspirin or sodium salicylate. Aspirin and sodium salicylate are equipotent inhibitors of IKKβ (*2*), whereas aspirin is ~100-fold more potent toward the cyclooxygenases (*21*). Our findings suggest that IKKβ, and not COX1 nor COX2, might alter insulin signaling. Additional NSAIDs were used to further evaluate potential molecular mediators. Ibuprofen and naproxen, which inhibit both COX1 and COX2, did not reverse TNF-α–induced insulin resistance (Fig. 4C). The selective COX2 inhibitor NS-398 similarly had no effect. Studies were conducted with doses of the drugs known to have biological effects (*2*, *21*). These pharmacological profiles further point to IKK as the target of these effects and demonstrate that COX1 and COX2, the classical targets for NSAIDs, do not mediate the antidiabetic effects of aspirin and salicylate. This issue was addressed further using mice with reduced COX expression; homozygous and heterozygous deletions of either COX1 or COX2 had no effect on carbohydrate or lipid metabolism in insulin-resistant mice (*22*).

IKK complexes contain the heterodimeric kinases IKKα and IKKβ and the scaffolding protein IKKγ (*14*). Either the IKKβ catalytic

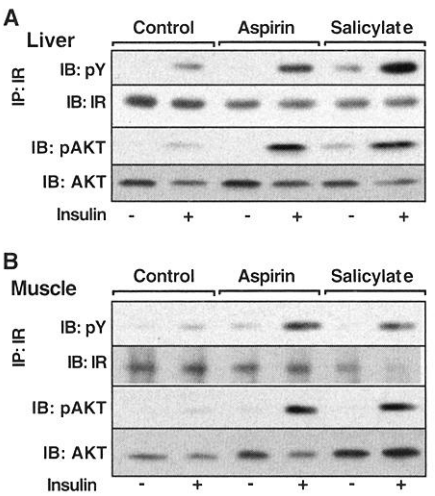

Fig. 2. Signaling proteins in tissues from aspirin- and salicylate-treated Zucker *fa/fa* fatty rats. Animals treated for 3 to 4 weeks with aspirin or sodium salicylate received intravenous injections of insulin or saline 7 min before being killed. Tissues were harvested and frozen immediately in liquid nitrogen. Liver and plantaris muscle samples were homogenized and signaling proteins were identified by Western blotting (*13*). (**A**) Liver or (**B**) muscle homogenates were immunoprecipitated with antiIR and proteins were identified by blotting with anti-pY and anti-IR. Alternatively, tissue homogenates were separated by SDS-PAGE and proteins were identified by blotting with antibodies specific to phospho-AKT (pAKT) and antibodies to AKT. IB, immunoblot; IP, immunoprecipitate.

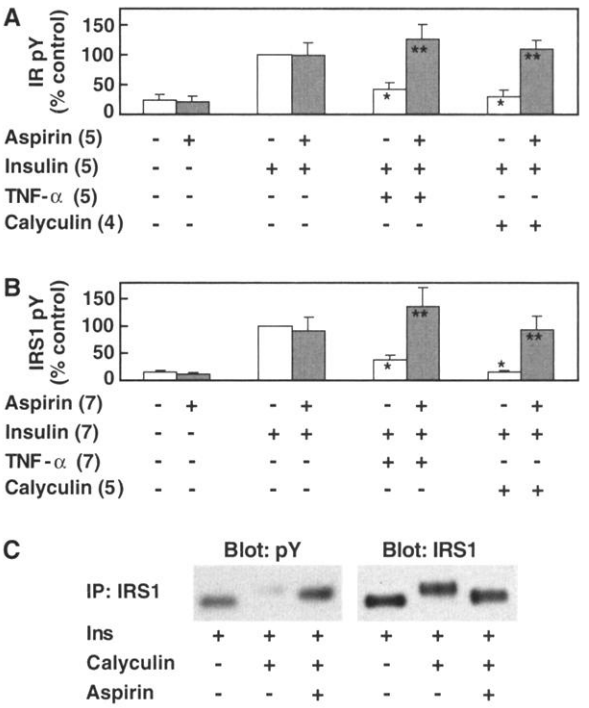

Fig. 3. Aspirin effects on insulin signaling in 3T3-L1 adipocytes. 3T3-L1 adipocytes were serum-starved for 16 hours and treated or not treated with 5 mM aspirin for 2 hours and either 6.0 nM mTNF-α (20 min) or the phosphatase inhibitor calyculin A (at 2.0 nM for 30 min). After a 5-min stimulation with 10 nM insulin, the cells were chilled and solubilized and proteins were immunoprecipitated with (**A**) anti-IR or (**B** and **C**) anti-IRS1. Proteins separated by SDS-PAGE were identified by Western blotting with anti-pY, anti-IR, or anti-IRS1. Control blots (not shown) indicated that protein amounts of IR and IRS1 did not differ significantly between treatments. Ins, insulin. (A and B) Phosphorylation levels were quantified by densitometry and expressed relative to insulin-stimulated controls; the numbers of individual experiments are shown in parentheses (*$P < 0.01$ for minus aspirin, plus insulin, minus versus plus mTNF-α, or minus versus plus calyculin A; **$P < 0.05$ for minus versus plus aspirin of mTNF-α or calyculin A–treated pairs; Student's t test).

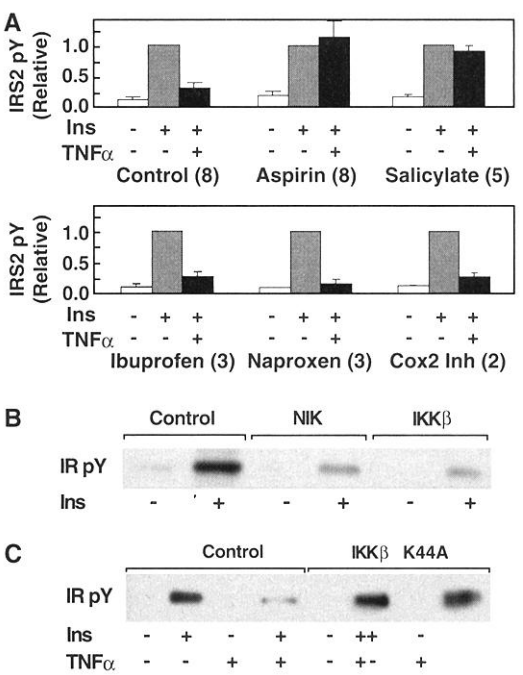

Fig. 4. (**A**) NSAID effects in Fao hepatoma cells. Fao cells were serum-starved for 16 hours followed by 2-hour incubations at 37°C with 5 mM aspirin, 10 mM sodium salicylate, 25 μM ibuprofen, 25 μM sodium naproxen, or 25 μM NS-398 (a selective COX2 inhibitor). Cells were then stimulated sequentially with 6.0 nM mTNF-α for 20 min and 10 nM insulin for 5 min. Cells were chilled and solubilized and proteins were immunoprecipitated with anti-IR and detected by Western blotting using anti-pY. Phosphorylation was quantified by densitometry and is expressed relative to insulin-stimulated controls; the numbers of individual experiments are shown in parentheses. (**B** and **C**) Induction of insulin resistance with IκB kinases and reversal with dominant inhibitors. (B) Myc-tagged NIK or Flag-tagged IKKβ or (C) kinase-deficient IKKβ were expressed in HEK 293 cells. The pRK7 (cytomegalovirus) vectors encoding the kinases were obtained from M. Rothe (Tularik); transfections of 50 to 60% confluent cells (1.5 μg of DNA per well; six well dishes) using FuGene 6 (Boehringer-Mannheim) were as recommended. Experiments were initiated 36 hours after transfection and 16 hours after removal of serum from the culture medium. (B) Cells were stimulated for 5 min with 10 nM insulin unless otherwise indicated. (C) Cells were treated for 40 min with 6 nM mTNF-α, followed by 5-min stimulations with 10 nM insulin. In (B) and (C), protein expression levels ranged from 10 to 20 times that of the endogenous proteins.

subunit or NIK, an upstream activator, was expressed in HEK 293 cells. Insulin stimulated the activation of IR (Fig. 4B), IRS-2, and AKT (*19*); activation was attenuated by expression of IKKβ or NIK (Fig. 4B) [Web fig. 2 (*11*)], and attenuated activation was reversed by treatment with aspirin (*19*). IκBα levels were reduced by IKKβ or NIK expression [Web fig. 2 (*11*)]. Because IKKα and IKKβ form heterodimers, overexpression of kinase-deficient IKKα or IKKβ inhibits endogenous components of the complex and signaling to NF-κB (*23*). We therefore asked whether the expression of dominant inhibitory IKKβ(K44A) blocked the induction of insulin resistance. TNF-α treatment reduced insulin-stimulated IR activation to 29 ± 2% of untreated controls, and expression of IKKβ(K44A) reversed the TNF-α–inhibited effects (Fig. 4C) [Web fig. 2 (*11*)]. Active IKKβ thus promotes insulin resistance in cultured cells, and the inactive, dominant inhibitory kinase blocks TNF-α induced insulin resistance.

Studies with mice having targeted disruption of the *Ikk*β locus further tested potential roles of IKKβ in the development and reversal of insulin resistance. *Ikk*$\beta^{-/-}$ mice die in utero because of enhanced liver apoptosis, whereas heterozygous *Ikk*$\beta^{+/-}$ mice were reportedly normal (*24*, *25*). Fasting glucose and insulin concentrations were consistently lower in *Ikk*$\beta^{+/-}$ compared to *Ikk*$\beta^{+/+}$ littermates (Fig. 5, A and B). The potential protective effect of reduced *Ikk*β gene dose was tested in crosses between *Ikk*$\beta^{+/-}$ and *Lep*$^{ob/ob}$ mice. Fasting blood glucose concentrations were reduced in *Ikk*$\beta^{+/-}$*Lep*$^{ob/ob}$ mice compared with those in *Ikk*$\beta^{+/+}$*Lep*$^{ob/ob}$ littermates (Fig. 5C). Glucose tolerance in the *Ikk*$\beta^{+/-}$*Lep*$^{ob/ob}$ mice was improved compared to *Ikk*$\beta^{+/+}$*Lep*$^{ob/ob}$ littermates (Fig. 5D), although insulin concentrations were indistinguishable (*12*). These findings are consistent with improved insulin sensitivity in *Ikk*$\beta^{+/-}$*Lep*$^{ob/ob}$ mice compared to that in *Ikk*$\beta^{+/+}$*Lep*$^{ob/ob}$ littermates. Also consistent with improved metabolic control, plasma FFA concentrations were lower in the *Ikk*$\beta^{+/-}$*Lep*$^{ob/ob}$ mice (1.86 ± 0.12 mM) than their *Ikk*$\beta^{+/+}$*Lep*$^{ob/ob}$ littermates (2.24 ± 0.09 mM; $P = 0.03$).

To further assess the effect of a reduction in *Ikk*β gene dose, mice were fed a diet high in fat. Fasting glucose and insulin concentrations were consistently lower in *Ikk*$\beta^{+/-}$ compared to *Ikk*$\beta^{+/+}$ littermates (Fig. 5, E and F). Reduced insulin concentrations in the *Ikk*$\beta^{+/-}$ mice were maintained throughout glucose tolerance testing in 18-week-old littermates (Fig. 5H). Dietary intake and weights were indistinguishable between all pairs of *Ikk*$\beta^{+/-}$ and *Ikk*$\beta^{+/+}$ littermates. These data demonstrate that a reduction in *Ikk*β gene dose reduces fasting glucose and insulin concentrations and protects against the development of insulin resistance in predisposed rodents.

Our findings demonstrate that increased IKK activity promotes insulin resistance, in obese rodents (*12*) when the kinase is overexpressed, or when IKK is activated by known stimulators. Conversely, reductions either in IKK activity or in the expression of its IKKβ subunit significantly improved insulin sensitivity. Even a 50% reduction in gene dosage improved in vivo glucose and lipid metabolism, which may explain why weak inhibitors of IKKβ, such as aspirin and sodium salicylate, have significant effects on glucose and lipid homeostasis. Although not recognized previously, there is an overlap between stimuli that activate IKK and conditions that promote insulin resistance, including proinflammatory cytokines such as TNF-α, hyperglycemia, phorbol esters and protein kinase C (PKC) enzymes, Ser-Thr phosphatase inhibitors, and bacterial lipopolysaccharide. These are either in vivo mediators of insulin resistance or experimental mimics in

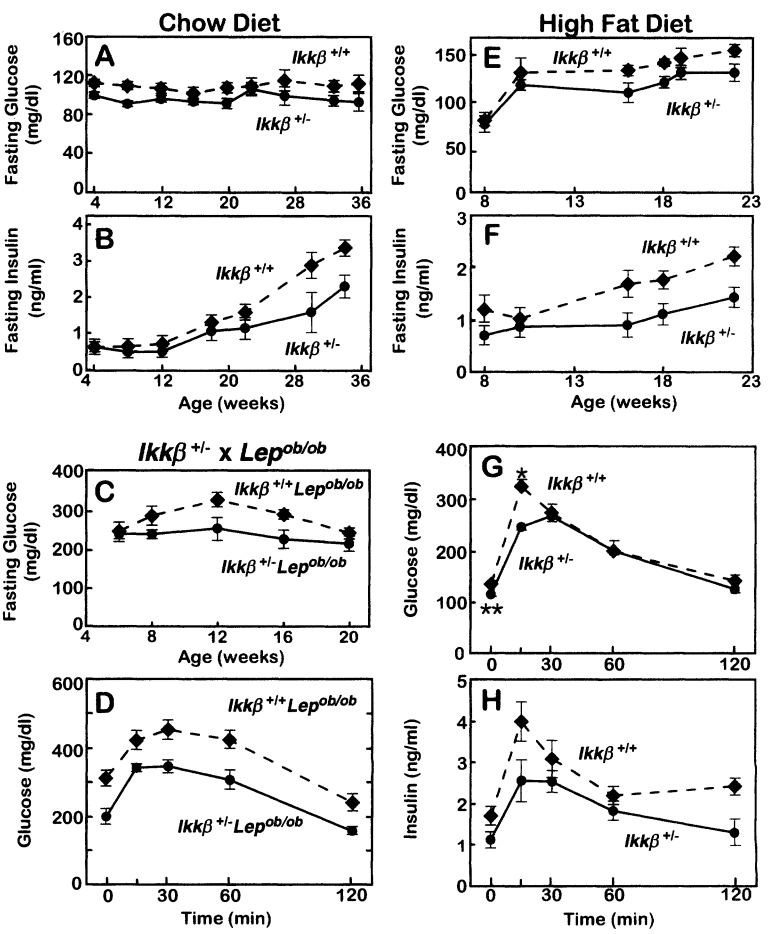

Fig. 5. Glucose tolerance and insulin sensitivity in *Ikk*$\beta^{+/-}$ mice. (**A** and **B**) *Ikk*$\beta^{+/-}$ mice were backcrossed four generations on a C57BL/6J background. Fasting blood glucose and fasting insulin concentrations were determined in *Ikk*$\beta^{+/-}$ and *Ikk*$\beta^{+/+}$ male littermates. Values represent the mean ± SEM for wild-type (WT) (diamonds, $n = 9$) and *Ikk*$^{+/-}$ (circles, $n = 6$) mice. (A) $P < 0.001$ and (B) $P = 0.02$ for integrated areas under the curves, Student's t tests for WT versus *Ikk*$^{+/-}$ mice. (**C** and **D**) *Ikk*$\beta^{+/-}$ offspring were crossed with *Lep*$^{ob/+}$ (C57BL/6J) mice (Jackson Laboratory, Bar Harbor, ME). F_1 male *Ikk*$^{+/-}$*Lep*$^{ob/+}$ offspring were crossed with *Ikk*$^{+/+}$*Lep*$^{ob/+}$ females, and F_2 littermates were studied. (C) Fasting blood glucose concentrations in male littermates. Values represent the mean ± SEM for *Ikk*$^{+/+}$*Lep*$^{ob/ob}$ (diamonds, $n = 7$) and *Ikk*$^{+/-}$*Lep*$^{ob/ob}$ (circles, $n = 7$); $P = 0.003$ for integrated areas under the curves; Student's t tests, *Ikk*$^{+/-}$*Lep*$^{ob/ob}$ versus *Ikk*$^{+/+}$ *Lep*$^{ob/ob}$. (D) Glucose tolerance tests were conducted with 9- to 12-week-old male *Ikk*$^{+/-}$*Lep*$^{ob/ob}$ and *Ikk*$^{+/+}$*Lep*$^{ob/ob}$ littermates. Glucose (2.0 g/kg) was administered by intraperitoneal injection after an overnight fast. Values represent the mean ± SEM for *Ikk*$^{+/+}$*Lep*$^{ob/ob}$ (diamonds, $n = 12$ males) and *Ikk*$^{+/-}$ *Lep*$^{ob/ob}$ (circles, $n = 11$ males; $P = 0.006$ for integrated areas under the curves; Student's t tests, *Ikk*$^{+/-}$*Lep*$^{ob/ob}$ versus *Ikk*$^{+/+}$*Lep*$^{ob/ob}$). (**E** to **H**) Beginning at 4 weeks of age, male *Ikk*$\beta^{+/-}$ and *Ikk*$\beta^{+/+}$ littermates were maintained on high-fat diets (Research Diets D12331; 58% of calories from coconut oil). Fasting (E) glucose and (F) insulin concentrations were measured from 8- to 23-week-old male littermates (diamonds, $n = 7$ *Ikk*$^{+/+}$ and circles, $n = 8$ *Ikk*$^{+/-}$ mice. (E) $P < 0.05$ and (F) $P = 0.01$ for integrated areas under the curves, Student's t tests for WT versus *Ikk*$^{+/-}$ mice. (G and H) Glucose tolerance tests were conducted with 18-week-old male littermates. Values represent the mean ± SEM for *Ikk*$^{+/+}$ (diamonds, $n = 10$) and *Ikk*$^{+/-}$ (circles, $n = 10$). (G) *$P < 0.005$; **$P < 0.01$, Student's t tests for WT versus *Ikk*$^{+/-}$ mice. (H) $P = 0.03$ for integrated areas under the curves, Student's t tests for WT versus *Ikk*$^{+/-}$ mice.

cultured cells. Our findings are consistent with potential links between chronic subacute inflammation and insulin resistance (*26*, *27*), whether this is mediated by TNF-α produced in fat (*28*–*31*) or through TNF-α–independent mechanisms. As a potentially important example of the latter, in rodent muscle, FFA infusion activates PKC-θ (*32*), a known activator of IKK (*33*), and FFA-induced insulin resistance is suppressed by aspirin treatment and in *Ikkβ*$^{+/-}$ mice (*34*). IKK activation through any mechanism initiates NF-κB–mediated transcription, which in certain cells would enhance the production of TNF-α. This positive feedback loop could perpetuate a vicious cycle of low-level inflammatory signaling, leading to insulin resistance. Our findings predict that IKK inhibition breaks this cycle. Too few tools are currently available to treat patients with insulin resistance and type 2 diabetes; IKKβ may provide a valuable target for the discovery of new drugs to treat these conditions.

References and Notes

1. E. Kopp, S. Ghosh, *Science* **265**, 956 (1994).
2. M. J. Yin, Y. Yamamoto, R. B. Gaynor, *Nature* **396**, 77 (1998).
3. W. Ebstein, *Berl. Klin. Wochnschr.* **13**, 337 (1876).
4. R. T. Williamson, *Br. Med. J.* **1**, 760 (1901).
5. J. Reid, A. I. Macdougall, M. M. Andrews, *Br. Med. J.* **2**, 1071 (1957).
6. S. G. Gilgore, *Diabetes* **9**, 392 (1960).
7. S. H. Baron, *Diabetes Care* **5**, 64 (1982).
8. Harvested liver and plantaris muscle samples were powdered under liquid nitrogen and homogenized in ice-cold buffer [30 mM Hepes (pH 7.4), 150 mM NaCl, 10% glycerol, 1% Triton X-100, 1 mM phenylmethylsulfonyl fluoride (PMSF), 3 μM aprotinin, 10 μM leupeptin, 5 μM pepstatin A, 25 mM benzamidine, 2 mM sodium orthovanadate, 5 mM β-glycerolphosphate, 100 mM NaF, 1 mM ammonium molybdate, 30 mM tetrasodium pyrophosphate, and 5 mM EGTA] for 30 s with a polytron. After centrifugation, proteins of interest were immunoprecipitated from supernatant solutions, separated by SDS–polyacrylamide gel electrophoresis (SDS-PAGE), and identified by Western blotting. In some cases, immunoprecipitated IRS-1 was treated with alkaline phosphatase (Boehringer-Mannheim; 60 U per 100-μl sample) for 60 min before separation by SDS-PAGE and Western blotting.
9. J. F. Caro, L. G. Dohm, W. J. Pories, M. K. Sinha, *Diabetes Metab. Rev.* **5**, 665 (1989).
10. L. J. Goodyear *et al.*, *J. Clin. Invest.* **95**, 2195 (1995).
11. Supplementary Web material is available on *Science* Online at www.sciencemag.org/cgi/content/full/293/5535/1673/DC1.
12. J. Lee, M. Yuan, L. Hansen, S. E. Shoelson, unpublished data.
13. Murine 3T3-L1 fibroblasts (American Type Culture Collection) were maintained in Dulbecco's modified Eagle's medium (DMEM) containing 25 mM glucose and 10% calf serum under 5% CO_2 in air. Confluent monolayers were differentiated into adipocytes by treatment for 3 days with DMEM containing 10% fetal bovine serum (FBS), insulin (10 μg/ml), 1.0 mM dexamethasone, and 0.5 mM isobutyl-1-methylxanthine under 10% CO_2. Cells were returned to DMEM containing 10% FBS and used for experiments 8 to 13 days after the initiation of differentiation. Before these experiments, differentiated 3T3-L1 adipocytes were serum-starved for 16 hours in DMEM containing 0.1% bovine serum albumin (BSA). Stocks (1.0 M) of acetylsalicylic acid (ASA) in 1.0 M tris-HCL were freshly prepared and pH was corrected to 7.4. Adipocytes were pretreated with 5 or 10 mM ASA for 2 hours at 37°C and then treated with either 6 nM murine TNF-α (mTNF-α) for 20 min, 2 nM calyculin A for 30 min, or 1 nM okadaic acid for 30 min at 37°C. Cells were stimulated with 10 or 100 nM insulin for 5 min at 37°C, washed twice with ice-cold Hepes buffer (25 mM, pH 7.4) containing 10% Earl's balanced salt solution (Gibco) and 0.1% BSA, and solubilized in tris-HCl buffer (50 mM, pH 7.4) containing 0.1% Triton X-100, 0.25% deoxycholate, 150 mM NaCl, 1 mM EGTA, 2 mM sodium orthovanadate, 100 mM NaF, 30 mM pyrophosphate, and freshly added protease inhibitors [1 mM PMSF, trasylol (1 μg/ml), leupeptin (1 μg/ml), and pepstatin (1 μg/ml)]. The cell lysates were clarified; equivalent amounts of proteins were precipitated with antibodies to IR (anti-IR) or antibodies to IRS1 (anti-IRS1) coupled to protein G–agarose, separated by SDS-PAGE under reducing conditions, transferred to PVDF membranes, and detected by immunoblotting with the relevant antibodies: antibody to phosphotyrosine (4G10; anti-pY) or COOH-terminally directed polyclonal anti-IR or anti-IRS1, followed by horseradish peroxidase (HRP)–conjugated second antibody to rabbit. The bands were visualized with enhanced chemiluminescence and quantified by scanning densitometry.
14. M. Karin, M. Delhase, *Semin. Immunol.* **12**, 85 (2000).
15. J. A. DiDonato, M. Hayakawa, D. M. Rothwarf, E. Zandi, M. Karin, *Nature* **388**, 548 (1997).
16. E. W. Harhaj, S. C. Sun, *J. Biol. Chem.* **272**, 5409 (1997).
17. K. A. Robinson, K. P. Boggs, M. G. Buse, *Am. J. Physiol.* **265**, E36 (1993).
18. K. Paz *et al.*, *J. Biol. Chem.* **272**, 29911 (1997).
19. N. Konstantopoulos, S. E. Shoelson, unpublished data.
20. Fao hepatoma cells, grown to 80% confluency, were serum-starved for 16 hours at 37°C in RPMI media containing 0.1% BSA. Stock solutions of 1.0 M aspirin and 1.0 M sodium salicylate were freshly prepared in 1.0 M tris-HCl (pH 7.4); stock solutions of 10 mM ibuprofen, 10 mM naproxen, and 10 mM NS-398 (Biomol, Plymouth, PA) were freshly prepared in ethanol.
21. D. E. Furst, *Arthritis Rheum.* **37**, 1 (1994).
22. *Cox1*$^{-/-}$ or *Cox2*$^{-/-}$ and *Lep*$^{ob/+}$ mice were crossbred to generate *Cox1*$^{+/-}$*Lep*$^{ob/ob}$, *Cox1*$^{-/-}$*Lep*$^{ob/ob}$, *Cox2*$^{+/-}$*Lep*$^{ob/ob}$, and *Cox2*$^{-/-}$*Lep*$^{ob/ob}$ mice (M. Yuan, L. Hansen, S. E. Shoelson, unpublished data).
23. E. Zandi, D. M. Rothwarf, M. Delhase, M. Hayakawa, M. Karin, *Cell* **91**, 243 (1997).
24. Q. Li, D. Van Antwerp, F. Mercurio, K. F. Lee, I. M. Verma, *Science* **284**, 321 (1999).
25. Z. W. Li *et al.*, *J. Exp. Med.* **189**, 1839 (1999).
26. J. C. Pickup, M. A. Crook, *Diabetologia* **41**, 1241 (1998).
27. A. Festa *et al.*, *Circulation* **102**, 42 (2000).
28. C. H. Lang, C. Dobrescu, G. J. Bagby, *Endocrinology* **130**, 43 (1992).
29. G. S. Hotamisligil, N. S. Shargill, B. M. Spiegelman, *Science* **259**, 87 (1993).
30. R. Feinstein, H. Kanety, M. Z. Papa, B. Lunenfeld, A. Karasik, *J. Biol. Chem.* **268**, 26055 (1993).
31. G. S. Hotamisligil, A. Budavari, D. Murray, B. M. Spiegelman, *J. Clin. Invest.* **94**, 1543 (1994).
32. M. E. Griffin *et al.*, *Diabetes* **48**, 1270 (1999).
33. Z. Sun *et al.*, *Nature* **404**, 402 (2000).
34. J. K. Kim *et al.*, *J. Clin. Invest.* **108**, 437 (2001).

35. This manuscript is dedicated to the memory of Shirley Blauner. We thank T. Maratos-Flier for helpful discussions and J. Warram for assistance with statistical analyses. Supported by NIH grants DK51729 (S.E.S.), DK45493 (S.E.S.), and AI43477 (M.K.); a research grant (S.E.S.) and a Mentor-Based Fellowship (M.Y. and N.K.) from the American Diabetes Association; the Cancer Research Institute (Z.W.L.); an American Cancer Society Research Professorship (M.K.); and a Burroughs Wellcome Fund Scholar Award in Experimental Therapeutics (S.E.S.).

12 April 2001; accepted 12 June 2001

Afterimage of Perceptually Filled-in Surface

Shinsuke Shimojo,[1,2]* Yukiyasu Kamitani,[1] Shin'ya Nishida[2]

An afterimage induced by prior adaptation to a visual stimulus is believed to be due to bleaching of photochemical pigments or neural adaptation in the retina. We report a type of afterimage that appears to require cortical adaptation. Fixating a neon-color spreading configuration led not only to negative afterimages corresponding to the inducers (local afterimages), but also to one corresponding to the perceptually filled-in surface during adaptation (global afterimage). These afterimages were mutually exclusive, undergoing monocular rivalry. The strength of the global afterimage correlated to a greater extent with perceptual filling-in during adaptation than with the strength of the local afterimages. Thus, global afterimages are not merely by-products of local afterimages, but involve adaptation at a cortical representation of surface.

Stimuli such as the one shown in Fig. 1A (left) (Varin configuration) induce vigorous perceptual color spreading, or filling-in (*1*–*3*), allegedly indicating some activation-spreading or completion mechanism in the cortical map (*4*–*6*). Fixating this stimulus leads to afterimages of the local inducers, i.e., the Pacmen/wedges or disks (Fig. 1B, left and center). An observer can also see a global afterimage of the perceptually filled-in surface (the large colored rectangle in this case) whose apparent color is complementary to that of the filled-in surface during the adaptation (Fig. 1B, right) as the opponent color theory predicts (*7*). This observation, together with the data reported below, suggests that cortical global processes and their adaptation are critical com-

[1]California Institute of Technology, Division of Biology, Computation and Neural Systems, Pasadena, CA, 91125, USA. [2]NTT Corporation, NTT Communication Science Laboratories, Human and Information Science Laboratory, Atsugi, Kanagawa, 243-0198, Japan.

*To whom correspondence should be addressed. E-mail: sshimojo@its.caltech.edu